International Journal of Advanced Research in Biological Sciences
ISSN: 2348-8069
www.ijarbs.com

Research Article

# Studies on preparation of $TiO_2$ Nanoparticles and its loaded groundnut shell activated carbon and their antibacterial activity

**S. Ragupathy and K. Raghu***

Department of Physics, Annamalai University, Annamalai Nagar, Chidambaram- 608 002, Tamilnadu, India.

*Corresponding author: *raghuk.phy@gmail.com*

**Abstract**

Preparation of titanium dioxide ($TiO_2$) nanoparticles and its loaded groundnut shell activated carbon ($TiO_2$/GNSAC) nanoparticles had been undertaken using sol-gel method and their application in antibacterial activity against human pathogens. The X-ray diffraction (XRD) pattern results reveal that the synthesized $TiO_2$ nanoparticles and $TiO_2$/GNSAC nanoparticles are in the tetragonal structure. The existence of functional groups was determined by Fourier transform infrared spectroscopy (FT-IR). The surface morphology of samples was studied by scanning electron microscope (SEM). We confirmed that the synthesized $TiO_2$/GNSAC have an effective antibacterial activity against *V. cholerae* bacteria than GNSAC and $TiO_2$ nanoparticles.

**Keywords:** $TiO_2$, $TiO_2$/GNSAC, Antibacterial activity

## Introduction

Antibacterial activity agents are very important in the textile industry, water disinfection, medicine and food packaging. Organic compounds are used for disinfection but some disadvantages, including toxicity to the human body, therefore the interest in inorganic disinfectants such as metal oxide nanoparticles is increasing (Hajipour *et al*., 2012). Nanoparticles are classified majorly into two types *viz*., organic and inorganic nanoparticles. The nanoparticles of carbon are called the organic nanoparticles. Magnetic nanoparticles, noble metal nanoparticles (platinum, gold and silver) and semiconductor nanoparticles (titanium dioxide, zinc oxide and zinc sulfide) are classified as inorganic nanoparticles (Kathiresan and Asmathunisha, 2013). Many possibilities of applications in the areas of physics, chemistry, pharmacy, surface coating agents, textile sizing, agriculture, biochemistry and so on (Wu *et al*., 2003; Fortner *et al*., 2005; Li *et al*., 2005).

Surface properties of titanium nanotubes have attracted more and more attention because of their prospects in photocatalysts, antibacterial and solar cells. Among various phases of titania reported, anatase shows a better photocatalytic activity and antibacterial performance (Yang *et al*., 2005; Hu *et al*., 2006, Sakatani *et al*., 2006). Furthermore, Anatase $TiO_2$ was also found to possess an effective antibacterial property (Carp *et al*., 2004). A wide range of materials such as, $TiO_2$ (Akhavan, 2009), $SiO_2$ (Oh *et al*., 2006), $Al_2O_3$ (Chang *et al*., 2007), Zeolites (Inoue *et al*., 2002) and activated carbon fibers [Chen et al. 2005] were studied against antibacterial activity. In the present work, in order to study the antibacterial activity performance against *V. cholerae* human pathogens, we synthesized $TiO_2$ and $TiO_2$/GNSAC nanoparticles using sol-gel method.

## Materials and Methods

### Preparation of $TiO_2$ and $TiO_2$ loaded GNSAC nanoparticles

The titanium dioxide ($TiO_2$) was synthesized by sol-gel method at room temperature directly from titanium tetra isopropoxide ($C_{12}H_{28}O_4Ti$ assay ≥98%) and 2-propanol ($C_3H_8O$ assay >99%). 10 mL of titanium tetra isopropoxide was dissolved in 90 mL of 2-propanol. After stirring for 5 min at room temperature, 30 mL of water was added drop wise with vigorous stirring for 2 hrs to obtain a homogeneous gel which was then calcined at 500 °C for 2 hrs to obtain $TiO_2$. The $TiO_2$/GNSAC catalyst was prepared by a similar method by adding 2.8 g of GNSAC (50 wt% with regard to the $TiO_2$) to the titanium tetra isopropoxide 2-propanol solution. After stirring, the solution was filtered using whatman filter paper (11mm) and washed several times by ethanol and deionized water. The precipitate formed was dried at 100 °C for 5 hrs to evaporate water and organic residues and then ground using an agate mortar to avoid agglomeration. Finally the powder was calcinated at 500 °C in muffle furnace for 2 hrs to obtain $TiO_2$/GNSAC.

### Characterization

The functional groups were determined by Fourier transform infrared spectroscopy (FT-IR). Spectra of the samples were recorded using NICOLET AVATAR 330. The samples were scanned 16 times per minute and spectra were recorded in the region 4000–400$cm^{-1}$ with wave number accuracy of 0.01 $cm^{-1}$. The crystal structures and particle size of GNSAC, $TiO_2$ and $TiO_2$/GNSAC were analyzed by X-ray diffraction (XRD) measurement which was carried out by using XPERT-PRO diffractometer system using Cu-Kα radiation (λ = 1.5406Å), as in the 2θ range from 10 to 80°, operating at 30 mA and 40 kV. The morphology of the products was explored using scanning electron microscope JEOL: JSM-5610LV equipped with energy dispersive spectrometer (Bruker) at an accelerating voltage of 20 kV.

### Antibacterial activity test

The antibacterial activity of GNSAC, $TiO_2$ and $TiO_2$/GNSAC nanoparticles was tested against the bacterial pathogens using disc diffusion assay. The pathogens namely Vibrio cholerae was obtained from Raja Sir Muthaiya Medical College, Annamalai University. Whatman filter paper (No.1) disc of 6mm diameter were impregnated with 10µl of the solution containing GNSAC, $TiO_2$ and $TiO_2$/GNSAC obtained from a concentration of 100 mg/mL and these disc were evaporated at 37 °C for 24 hrs. References standard disc were prepared with Ampicillin (50 µg/mL) to compare the antibacterial activity results of GNSAC, $TiO_2$ and $TiO_2$/GNSAC. After drying, the disc with GNSAC, $TiO_2$ and $TiO_2$/GNSAC and Ampicillin were placed on Muller Hinton Agar (MHA) plates were the bacterial culture was swabbed on the surface of the agar and incubated for 24 hrs at 37 °C. After incubation, plates were examined for clear zone around the disc with GNSAC, $TiO_2$ and $TiO_2$/GNSAC and Ampicillin. A clear zone with diameter more than 2 mm was taken as an antibacterial activity and the results were expressed in mm. The plates were incubated at 37 °C for 24 hrs to measure zone of inhibition. The mean was calculated by performing the experiments in triplicates.

## Results and Discussion

### Fourier transform infrared spectroscopy (FT-IR)

Fig.1a-c shows the FT-IR spectra of GNSAC and $TiO_2$, $TiO_2$/GNSAC nanoparticles after calcination at 500 °C for 2 hrs. In Fig.1a for the groundnut shell activated carbon, of the sharp peak located at 2931 $cm^{-1}$ corresponds to aliphatic C-H stretching vibrations in methyl and methylene groups, while the band at 1599 $cm^{-1}$ to C=C stretching of aromatic group (Mahmoodi et al., 2011). The peak at 1188 $cm^{-1}$ is assigned to the stretching vibration P-O-C (aromatic) linkage and P=OOH (Hadoun *et al*., 2013). The broad band at 1300-900 $cm^{-1}$ in GNSAC has a maximum at 1078 $cm^{-1}$. The adsorption in this region is the characteristics for phosphorous. These bands arise as a result of phosphoric acid impregnation during GNSAC synthesis. Spectra of both $TiO_2$ and $TiO_2$/GNSAC are found to have significant hydroxyl groups on their surface.

A broad band is observed in between 3600 and 3000 $cm^{-1}$ is related to the O-H stretching mode of hydroxyl group, indicating the presence of moisture in the samples. The characteristic peak at 1633 $cm^{-1}$ is associated with the O-H bending vibrations of the absorbed water molecules. The two observed peaks at 3412 and 1633 $cm^{-1}$ correspond to the surface adsorbed water and hydroxyl groups (Praveen *el al*., 2014).

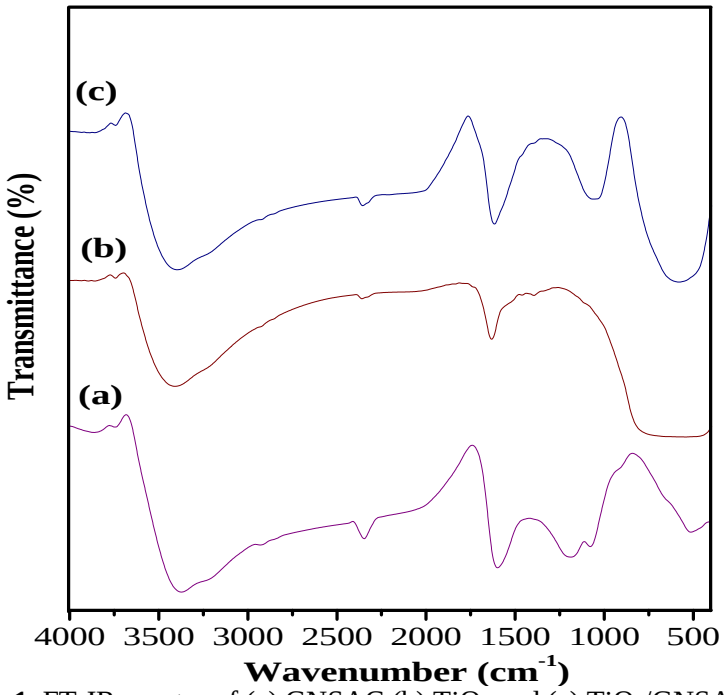


**Fig.1.** FT-IR spectra of (a) GNSAC (b) $TiO_2$ and (c) $TiO_2$/GNSAC.

A new peak at 1064 $cm^{-1}$ can be assigned to C-O stretching vibration. For the pure $TiO_2$, the broad peak at range from 800-400 $cm^{-1}$ is the contributions from the anatase titania. A broad absorption band between 800 and 450 $cm^{-1}$ region is ascribed to the vibration absorption of the Ti-O-Ti linkages in $TiO_2$/GNSAC (Lu *et al*., 2008). The FT-IR results, strongly confirm the presence of hydroxyl groups in the structure of the $TiO_2$/GNSAC.

**X-ray diffraction (XRD)**

The XRD patterns of the prepared $TiO_2$ and $TiO_2$/GNSAC nanoparticles calcination at 500 °C for 2 hrs and GNSAC are shown in Fig. 2a-c. Figure 2a the diffraction profile of GNSAC exhibits two broad peaks at 2θ = 26 and 43° which are similar to the peaks of crystalline carbonaceous structure and the absence of sharp peak reveals a predominantly amorphous structure.

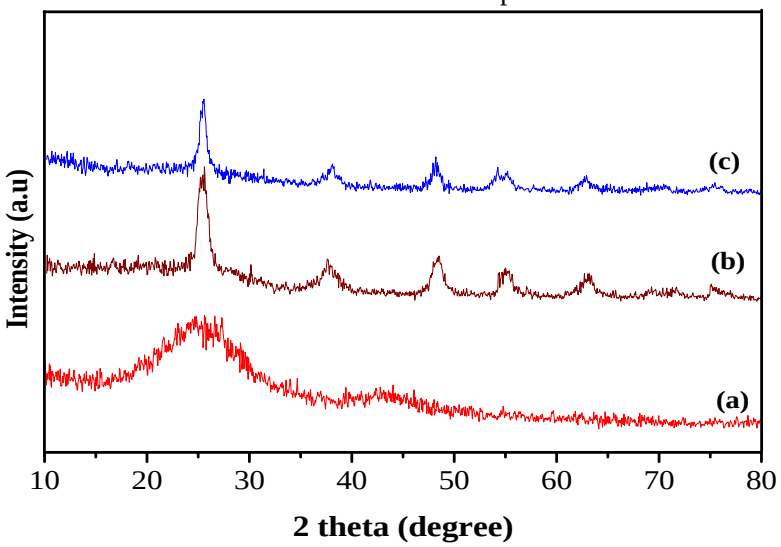


**Fig.2.** XRD patterns of (a) GNSAC (b) $TiO_2$ and $TiO_2$/GNSAC.

Fig.2b-c show sharp peaks exhibiting the crystalline nature of $TiO_2$ and $TiO_2$/GNSAC nanoparticles. X-ray diffraction studies indicate that the materials synthesized are pure anatase $TiO_2$ phase with the tetragonal structure. The obtained results are well agreed with the corresponding reported JCPDS value (Card No. 71-1166). Average particle size of $TiO_2$ and $TiO_2$/GNSAC nanoparticles are calculated using the Scherrer's formula given by,

$$D = \frac{K\lambda}{\beta \cos\theta} \qquad (1)$$

Where D is the average crystallite diameter (nm), K is the Scherrer's constant (0.9), λ is the wavelength (1.5406 Å), β is the Full width at half maximum, and θ is the Bragg angle. The average crystallite size of $TiO_2$ and $TiO_2$/GNSAC are calculated to be 18.79 and 8.7 nm, respectively. The XRD peaks exactly match with the anatase phase of $TiO_2$ showing that GNSAC modification does not change the phase. The broadening of peaks implies the decrease in crystalline size of $TiO_2$ (Jamil *et al*., 2012).

**Scanning electron microscopy (SEM)**

The surface morphology of GNSAC, $TiO_2$ and $TiO_2$/GNSAC nanoparticles are shown in Fig.3a-c. Pure $TiO_2$ is observed to exhibit surface particle agglomeration. GNSAC showed that the cavities on the surfaces of the carbon sample resulted from the evaporation of the $H_3PO_4$ during carbonization, leaving the space open that was previously occupied by $H_3PO_4$. During impregnation, the molecules of the chemical impregnating agent diffused into the texture of the lignocellulosic material. On carbonization at the desired temperature, the chemical impregnating agent evaporates and makes the remaining carbon texture porous (Alothman, 2013). $TiO_2$/GNSAC exhibits a rough porous surface resulting from the growth of $TiO_2$ nanoparticles on GNSAC surface.

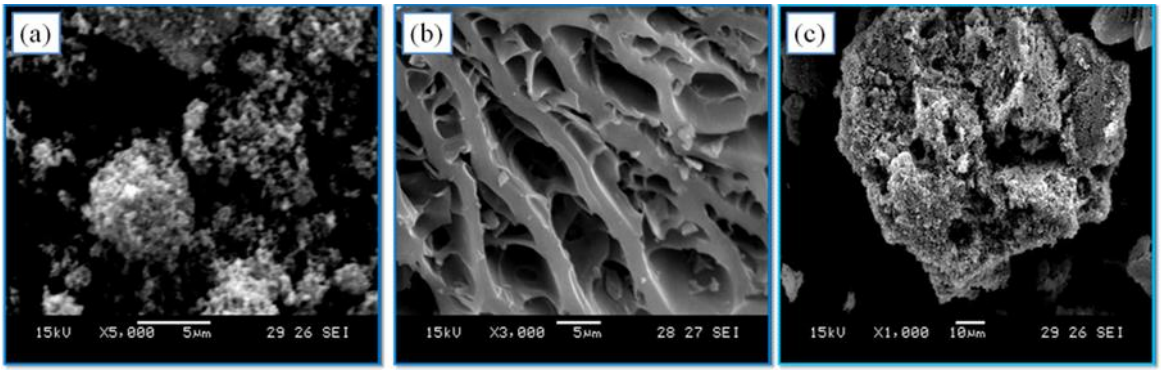


**Fig.3;** SEM images of (a) $TiO_2$, (b) GNSAC and (c) $TiO_2$/GNSAC.

**Antibacterial activity**

The results of the antibacterial activity of GNSAC, $TiO_2$, and $TiO_2$/GNSAC confirmed an antibacterial effect on the diameters of the inhibition zones. All samples were tested against Gram-negative (*V. cholerae*) bacteria. The GNSAC, $TiO_2$ and $TiO_2$/GNSAC were tested for its antibacterial activity using Muller Hinton Agar (MHA) plates, prepared by growing bacterial lawn of *V. cholerae*. Each plate referred to an individual samples as shown in Fig.4.

Each plate also had positive standard (S) and negative control (C). The positive standard (S) was ampicillin (50µg/ml) which is an antibiotics and the negative control (C) was 50 µl of DMF. The zone of sensitivity of conjugate was compared with the positive standard. Each disk was prepared containing 50 µl of samples and was placed on agar plate along with both positive standard and negative control incubated at 37 °C for 24 h. During the incubation period, the zones of inhibition were measured. It is apparent that the samples showed inhibition zone against almost the test organisms (Paskalis Sahaya Murphin Kumar *et al*., 2014) are shown in Table 1.

.

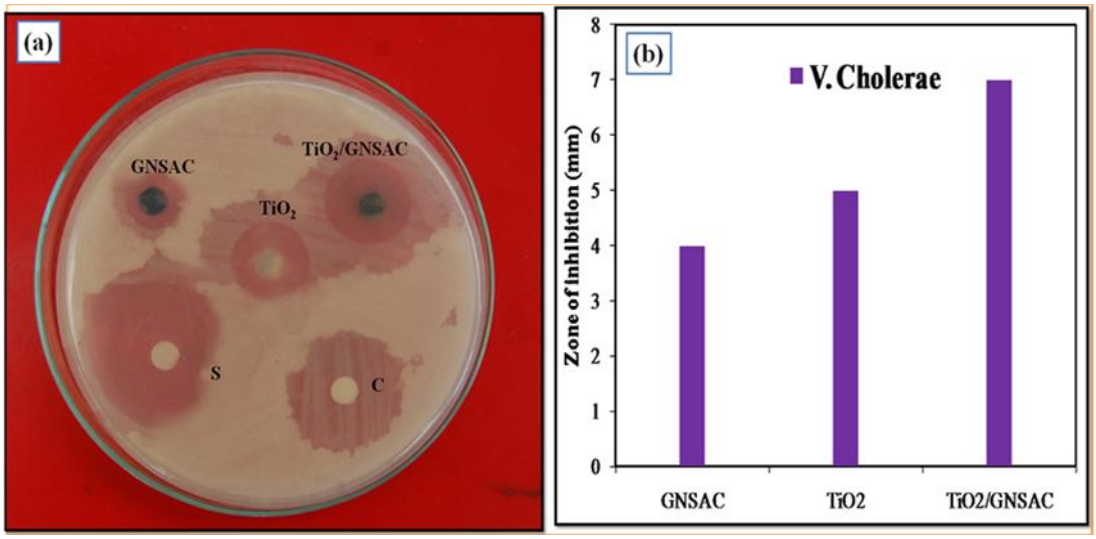


**Fig.4:** Antibacterial activity of GNSAC, $TiO_2$ and $TiO_2$/GNSAC, against (a) *V. cholerae* bacteria and (b) corresponding bar diagram.

**Table 1** Antibacterial activity of synthesized $TiO_2$ loaded GNSAC nanoparticles against human pathogens.

| Species | Zone of inhibition (mm) | | | |
|---|---|---|---|---|
| | GNSAC | $TiO_2$ | $TiO_2$/GNSAC | Standard (S) |
| *V. cholerae* | 4 | 5 | 7 | 13 |

In $TiO_2$/GNSAC (Fig. 4) showed that the maximum zone of inhibition was found against gram positive *V. cholerae* (7 mm) and it was higher than that of the positive standard ampicillin (13 mm).

## Conclusion

The antibacterial activity of $TiO_2$ and $TiO_2$/GNSAC nanoparticles were tested against gram positive bacteria *V. cholerae* using disc diffusion method. The $TiO_2$/GNSAC nanoparticles shows maximum zone of inhibition than GNSAC and $TiO_2$ nanoparticles. The higher antibacterial activity of $TiO_2$/GNSAC nanoparticles can be attributed due to reduced crystallite size and increased surface area.

## Acknowledgments

The authors wish to thank Dr. S. Barathan, The Professor and Head, Department of Physics, Annamalai University, for having provided the necessary laboratory facilities to carry out this work. The authors also thank Centralized Instrumentation and Services Laboratory (CISL), Annamalai University for providing their analytical instrument facilities.

## References

Akhavan, O., Lasting antibacterial activities of Ag–$TiO_2$/Ag/a-$TiO_2$ nanocomposite thin film photocatalysts under solar light irradiation, J. Colloid. Interface Sci. 336 (2009) 117–124.

Alothman, Z.A., Naushad, Mu, Rahmat Ali, Kinetic, equilibrium isotherm and thermodynamic studies of Cr (VI) adsorption onto low-cost adsorbent developed from peanut shell activated with phosphoric acid, Environ Sci. Pollut. Res., DOI 10.1007/s11356-012-1259–4, (2013).

Carp, O., Huisman, C.L., Reller, A., Photoinduced reactivity of titanium dioxide. Prog. Solid State Chem. 32 (2004) 33–177.

Chang, Q.Y., Yan, L.Z., Chen, M.X., He, H., Qu, J.H., Bactericidal mechanism of Ag/$Al_2O_3$ against Escherichia coli, Langmuir, 23 (2007) 11197–11199.

Chen, S.X., Liu, J.R., Zeng, H.M., Structure and antibacterial activity of silver supporting activated carbon fibers, J. Mater. Sci. 40 (2005) 6223–6231.

Fortner, J.D., Lyon, D.Y., Sayes, C.M., Boyd, A.M., Falkner, J.C., Hotze, E.M., et al., C-60 in water: Nanocrystal formation and microbial response. Environ. Sci. Technol. 39 (2005) 4307–4316.

Hadoun, H., Sadaoui, Z., Souami, N., Sahel, D., Toumert, I., Characterization of mesoporous carbon prepared from date stems by $H_3PO_4$ chemical activation, Appl. Surface Sci. 280 (2013) 1– 7.

Hajipour, M.J., Fromm, K.M., et al., Antibacterial properties of nanoparticles, Trends in Biotechnol. 30 (2012) 499–511.

Hu, C., Lan, Y., Hu, X., Wang, A., Ag/AgBr/$TiO_2$ visible light photocatalyst for destruction of azodyes and bacteria, J. Phys. Chem. B 110 (2006) 4066–4072.

Inoue, Y., Hoshino, M., Takahashi, H., Noguchi, T., Murata, T., Kanzaki, Y., Hamashima, H., Sasatsu, M., Bactericidal activity of Ag–Zeolite mediated by reactive oxygen species under aerated conditions, J. Inorg. Biochem. 92 (2002) 37–42.

Jamil, T.S., Ghaly, M.Y., Fathy, N.A., Abd el-halim, T.A., Osterlund, L., Enhancement of $TiO_2$ behavior on photocatalytic oxidation of MO dye using $TiO_2$/AC under visible irradiation and sunlight radiation, Sep. Purif. Technol. 98 (2012) 270–279.

Kathiresan, K., Asmathunisha, N., A review on biosynthesis of nanoparticles by marine organisms. Colloid. Surface B: Bio interfaces. 103 (2013) 283–287.

Li, P., Li, J., Wu, C., Wu, Q., Li, J., Synergistic antibacterial effects of lactam antibiotic combined with silver nanoparticles. Nanotechnol. 16 (2005) 1912–1917.

Lu, X., Lv, X., Sun, Z., Zheng, Y., Nanocomposites of poly (L-lactide) and surface-grafted $TiO_2$ nanoparticles: Synthesis and characterization, Eur. Polym. J. 44 (2008) 2476–2481.

Mahmoodi, N.M., Salehi, R., Arami, M., Binary system dye removal from colored textile wastewater using activated carbon: Kinetic and isotherm studies, Desalination, 272 (2011) 187–195.

Oh, S.D., Lee, S.H., Choi, S.H., Lee, I.S., Lee, Y.M., Chun, J.H., Park, H.J., Synthesis of Ag and Ag–$SiO_2$ nanoparticles by irradiation and their antibacterial and antifungal efficiency against Salmonella enterica serovar Typhimurium and Botrytiscinerea, Colloid Surf. A: Physicochem. Eng. Aspects, 275 (2006) 228–233.

Paskalis Sahaya Murphin Kumar, Arul Prakash Francis, Thiyagarajan Devasena, Biosynthesized and chemically synthesized titania nanoparticles: comparative analysis of antibacterial activity, J. Environ. Nanotechnol. 3 (2014) 73–81.

Praveen, P., Viruthagiri, G., Mugundan, S., Shanmugam, N., Structural, optical and morphological analyses of pristine titanium di-oxide nanoparticles–Synthesized via sol–gel route, Spectrochim. Acta A 117 (2014) 622–629.

Sakatani, Y., Grosso, D., Nicole, L., Boissiere, C., Illia, S., Sanchez, C., Optimised photocatalytic activity of grid-like mesoporous $TiO_2$ films: effect of crystallinity, pore size distribution and pore accessibillity, J. Mater. Chem. 16 (2006) 77–82.

Wu, X., Liu, H., Liu, J., Haley, K.N., Treadway, J.A., Larson, J.P., et al., Immunofluorescent labeling of cancer marker Her and other cellular targets with semiconductor quantum dots. Nat. Biotechnol. 21 (2003) 41–46.

Yang, S.W., Gao, L., Preparation of titanium dioxide nanocrystallite with high photocatalytic activities, J. Am. Ceram. Soc. 88 (2005) 968–970.